Journal of Materials Chemistry A

ROYAL SOCIETY OF CHEMISTRY

PAPER

View Article Online
View Journal | View Issue

Cite this: J. Mater. Chem. A, 2024, 12, 19513

Intramolecular assembly of dinitromethyl and bistetrazole: a strategy for constructing advanced and environmentally friendly high-energy density materials†

Xuezhi Yu,[a] Jie Tang,[a] Caijin Lei,[a] Chungui Xue,[a] Guangbin Cheng, *[a] Chuan Xiao*[b] and Hongwei Yang *[a]

Bistetrazoles have received extensive attention from researchers in the field of energetic materials due to their high heat of formation (ΔH_f = 4.06 kJ g^{-1}) and high nitrogen content (N% = 81.14%). In this work, target product 2,2′-bis(dinitromethyl)-2*H*,2′*H*-5,5′-bistetrazole (**BDNBT**), composed of dinitromethyl and bistetrazole, could significantly improve the dilemma of high sensitivity of bistetrazole-derived energetic materials. The two polymorphic forms (α and β) of **BDNBT** exhibit differences in density and detonation performance among other aspects. The polymorph α of **BDNBT** with near-zero oxygen balance (OB% = −4.62%) has a crystal density of up to 1.917 g cm^{-3} (193 K) and excellent detonation properties (D = 9480 m s^{-1} and P = 40.2 GPa), superior to those of polymorph β of **BDNBT** (ρ = 1.899 g cm^{-3} (193 K), D = 9306 m s^{-1}, and P = 38.5 GPa). In this study, five monovalent cationic salts (**4–8**) and two divalent cationic salts (**9–10**) of **BDNBT** were synthesised and discussed. Among them, energetic 2,4,6-triamino-1,3-dihydroxy-1,3,5-triazine-1,3-diium salts **10** exhibits superior detonation performance to RDX (D = 8795 m s^{-1} and P = 34.9 GPa) and HMX (D = 9144 m s^{-1} and P = 39.3 GPa), with a density of 1.904 g cm^{-3}, a detonation velocity of 9612 m s^{-1}, an impact sensitivity of 10 J and a friction sensitivity of 120 N. This work provides guidance for future researchers to develop high-energy density materials and enhance material properties through crystal phase transitions.

Received 22nd May 2024
Accepted 23rd June 2024

DOI: 10.1039/d4ta03537b

rsc.li/materials-a

Introduction

In the development of energetic materials, bistetrazole (H_2BT), as an early high energy material, has attracted much attention due to its high nitrogen content (N% = 81.14%) and high heat of formation (ΔH_f = 4.06 kJ g^{-1}). Energetic materials with high nitrogen content typically exhibit excellent detonation performance and environmental friendliness.[1–3] Therefore, a series of reactions based on bistetrazole have emerged in the past decade, leading to the synthesis of many high-performance bistetrazole derivatives, such as compounds **A–F** shown in Fig. 1.[1,4–8] The detonation performance is further improved by the introduction of two nitroamino groups on the N–H bond of bistetrazole in *N*,*N*′-(1*H*,1′*H*-[5,5′-bistetrazole]-1,1′-diyl)dinitramide (**A**), with a detonation velocity of up to 10 055 m s^{-1}.[3] Amino groups were introduced at different positions of bistetrazole to yield a group of structural isomers 1*H*,1′*H*-[5,5′-bistetrazole]-1,1′-diamine (**B**) and 1*H*,2′*H*-[5,5′-bistetrazole]-1,2′-diamine (**C**), which achieve a breakthrough in nitrogen content (N% = 83.31%). 1*H*,1′*H*-[5,5′-Bistetrazole]-1,1′-diol (**D**) has a high density of 1.953 g cm^{-3} due to the presence of hydroxyl groups.[6] Although all these compounds further leverage the advantages of high detonation velocity of bistetrazoles, they exhibit poor sensitivity and oxygen balance performance. The impact sensitivities of the above derivatives **A** to **F** are all less than 3 J, and friction sensitivities are all less than 5 N. Compared with RDX (FS = 120 N) and HMX (FS = 120 N), these derivatives exhibit a more significant disadvantage in terms of friction sensitivity.[6] Even with a high detonation velocity, highly sensitive bistetrazole derivatives cannot be practically utilized due to the significant safety risks.[9–12]

In order to achieve a better balance between energy and safety of energetic materials in the design of high-energy and low-sensitivity energetic materials today, three strategies are generally adopted to improve their overall performance: (1) introducing stabilizing groups containing hydrogen, such as amino groups or different hydrogen-containing nitrogen heterocyclic energetic groups, into the energetic framework to

[a]School of Chemistry and Chemical Engineering, Nanjing University of Science and Technology, Xiaolingwei 200, Nanjing, Jiangsu, China. E-mail: hyang@mail.njust.edu.cn; gcheng@mail.njust.edu.cn

[b]China Northern Industries Group Co., Ltd. (NORINCO GROUP), Beijing 100089, P. R. China. E-mail: 47785121@qq.com

† Electronic supplementary information (ESI) available. CCDC 2336247, 2336254–2336256, 2336263, 2336277, 2339222 and 2339223. For ESI and crystallographic data in CIF or other electronic format see DOI: https://doi.org/10.1039/d4ta03537b

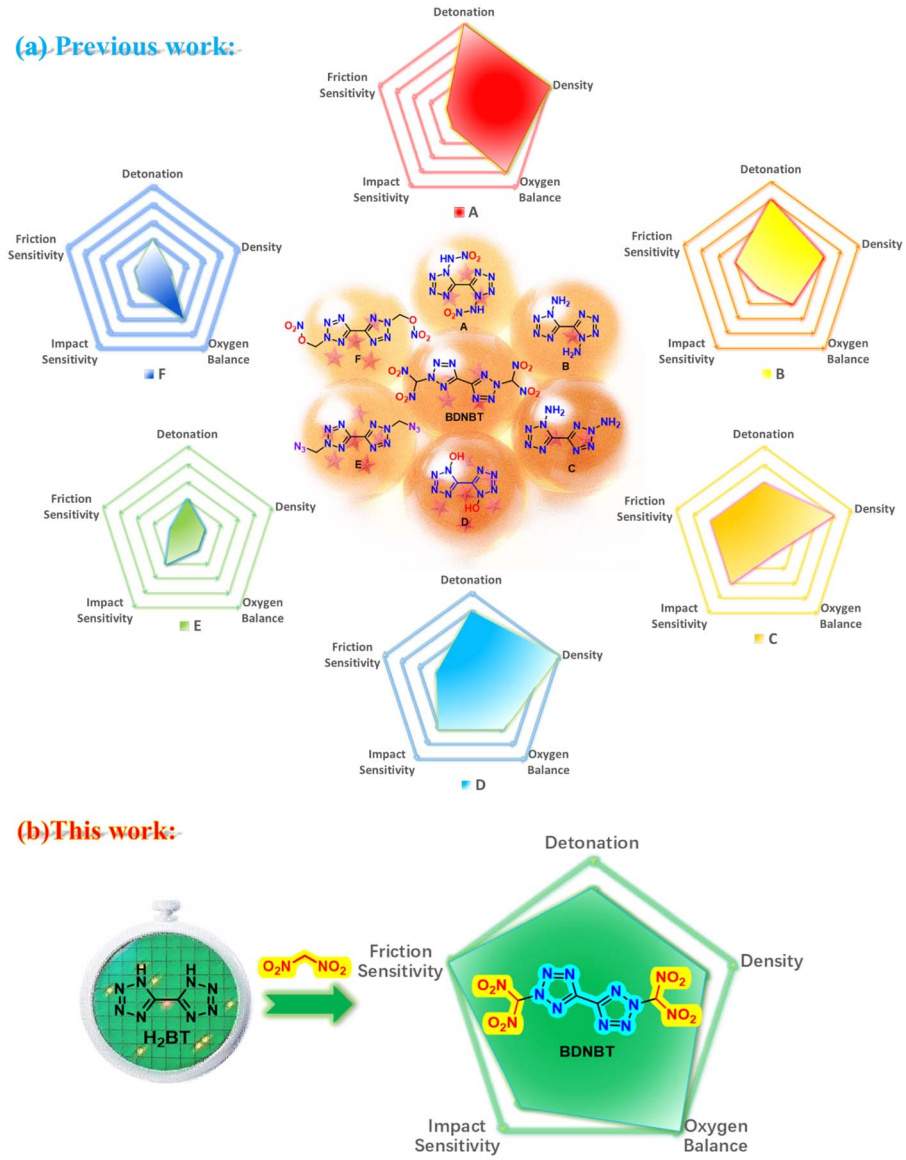

Fig. 1 (a) The structures of bistetrazole and its derivatives. (b) Target energy materials for the current study.

form highly stable multiple hydrogen bonding network structures; (2) optimizing the crystal structure of energetic compounds through microstructural control methods to create more stable and ordered packing forms; (3) constructing energetic ionic salts based on high-energy energetic cations and anions to enhance the stability of energetic materials. The above three efficient strategies were attempted to be applied in this study. Firstly, the introduction of dinitromethyl, a hydrogen-containing nitrogen heterocyclic high-energy group, is a highly efficient means of improving the overall performance of novel high-energy density materials (HEDMs).[13–16] In addition, introducing the planar dinitromethyl anion into nitrogen-containing rings facilitates the formation of a conjugated structure, thereby effectively increasing the density, oxygen balance, and detonation performance of energetic compounds.[17–19] Intramolecular assembly of dinitromethyl and bistetrazoles has been a major highlight of this work. Secondly, crystal phase transformation, as an efficient method to enhance the overall performance of energetic materials, involves orderly arrangement of molecules at the microscopic level to increase compound density and intermolecular forces. This in turn impacts properties such as detonation performance and thermal stability of materials. In this study, the polymorphic transformation from one crystal form into another was discussed for the target compound **BDNBT**. Thirdly, to fully leverage the advantage of a dinitromethyl anion in forming a conjugated structure to effectively enhance the stability of energetic compounds, five monovalent and two divalent cationic energetic salts were synthesized to study the differences in their comprehensive performance changes. Multinuclear NMR (^{1}H and ^{13}C), infrared spectra, elemental analysis, and differential scanning calorimetry (DSC) have been used to

characterize each compound. Compounds **BDNBT**, **4**, **5**, **7**, and **9** underwent crystal X-ray diffraction analysis.

Results and discussion

Synthesis

The synthetic route for preparing these energetic materials is illustrated in Scheme 1. The starting material, 1*H*,1′*H*-5,5′-bis(tetrazole) (H_2BT), was synthesized following literature methods.[20] Firstly, H_2BT forms a potassium salt in aqueous potassium hydroxide solution. Then, it undergoes a substitution reaction with bromoacetone in the N–H position under acetone reflux conditions. After completion of the reaction, filtration and washing gave bright white product **2** with a 2,2-substituent position. The filtrate was concentrated under reduced pressure, and filtered and washed with water to give a beige solid product **1** with 1,2-substitution. Interestingly, it was found that the yield of compound **2** (yield: 60%) with a 2,2-substituent position was nearly twice that of compound **1** (yield: 30%) with 1,2-substitution after several experiments. It is worth noting that compounds **1** and **2** are isomers with similar onset decomposition temperatures (**1**: T_d = 240 °C; **2**: T_d = 235 °C) but radically different onset melting points (**1**: T_m = 128 °C; **2**: T_m = 220 °C) (DSC plot in ESI Fig. S2†). This may be attributed to the symmetrical structure of compound **2**, which exhibits greater molecular polarity, a more compact molecular arrangement and higher lattice energy compared with compound **1**. Unexpectedly, dinitromethylammonium salt **3**, the nitration decomposition product of compound **1**, was synthesized instead of the desired nitration product, 1,2′-bis(dinitromethyl)-1*H*,2′*H*-5,5′-bitetrazole (**3-1**) under nitration conditions (nitric acid : sulfuric acid = 1 : 1). Subsequently, different nitration systems were tested (100% nitric acid, fuming nitric acid, acetic anhydride : nitric acid = 1 : 1, fuming sulfuric acid : fuming nitric acid = 1 : 1), but none of them successfully yielded the desired product **3-1**.

In contrast to compound **1**, the nitration of compound **2** proceeded successfully, yielding the target compound 2,2′-bis(dinitromethyl)-2*H*,2′*H*-5,5′-bistetrazole (**BDNBT**). Like compounds **E** and **F**, the larger size of the dinitromethyl group makes the overall steric hindrance of the compound at the 2-position less than that at the 1-position. As a result, the 2-position bistetrazole skeleton is easier to form. Surprisingly, different crystal types **α-BDNBT** and **β-BDNBT** can be obtained by using different temperatures to incubate the crystals. **BDNBT** forms α-type cubic crystals when a saturated methanol solution is allowed to slowly evaporate at room temperature, but β-type spike-like crystals are obtained when the saturated methanol solution is rapidly evaporated at 60 °C. Furthermore, heating the α-form crystals in saturated methanol solution to 60 °C and then stopping the heating will cause the precipitated crystals to transform into β-form crystals. Similarly, β-form crystals dissolved in saturated methanol and slowly evaporated at room temperature will also transform into α-form crystals. To further investigate the detonation performance of **BDNBT** as an anionic salt, the corresponding energetic salts **4–10** were synthesized with different ratios of cations to anions (compounds **4–8**, 2 : 1 or compounds **9**, **10**, 1 : 1). Addition of sodium hydroxide, potassium hydroxide, ammonia, hydrazine hydrate, and hydroxylamine to the acetonitrile solution of **BDNBT** gives compounds **4** (yield: 79%), **5** (yield: 88%), **6** (yield: 94%), **7** (yield: 72%), and **8** (yield: 84%), respectively. Considering that 3-(aminomethyl)-4,5-diamino-1,2,4-triazole could provide melting point for potential molten-cast explosives and that 2,4,6-triamino-1,3,5-triazine-1,3-dioxide exhibits a high density, the energetic 3-(aminomethyl)-4,5-diamino-1,2,4-triazol-1-ium salt **9** and energetic 2,4,6-triamino-1,3-dihydroxy-1,3,5-triazine-1,3-diium salt **10** were attempted to be synthesized. **BDNBT** and 3-(aminomethyl)-4,5-diamino-1,2,4-triazole or 2,4,6-triamino-1,3,5-triazine-1,3-dioxide were stirred in deionised water and the two corresponding divalent high-energy salts were prepared to give a yellow solid **9** (yield: 92%) and a white solid **10** (yield: 94%), respectively.

The occurrence of the decomposition product dinitromethylammonium salt **3** attracted our attention. Possible reaction processes for the synthesis of compound **3** from compound **1** with the 1,2-substituent group are illustrated in

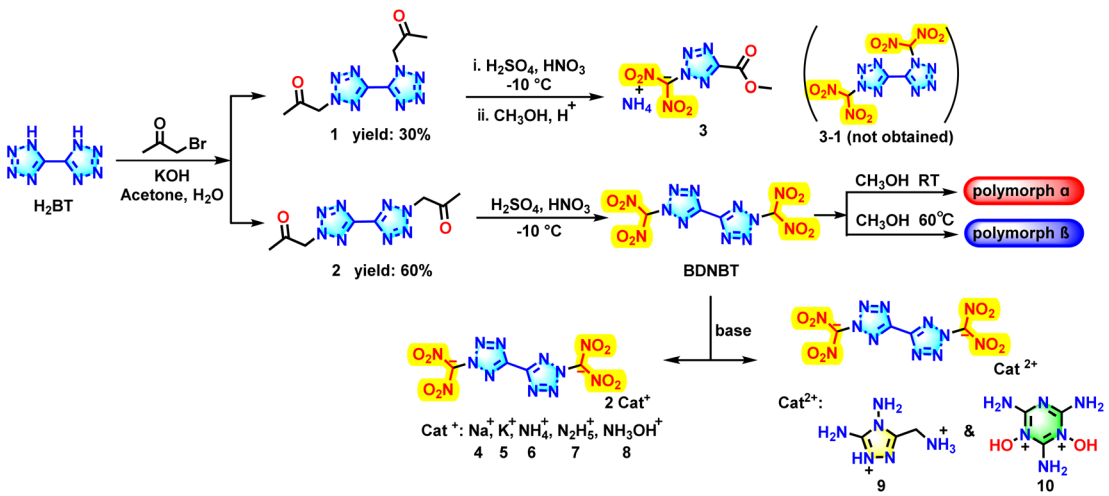

Scheme 1 Synthesis of BDNBT and compounds 3–10.

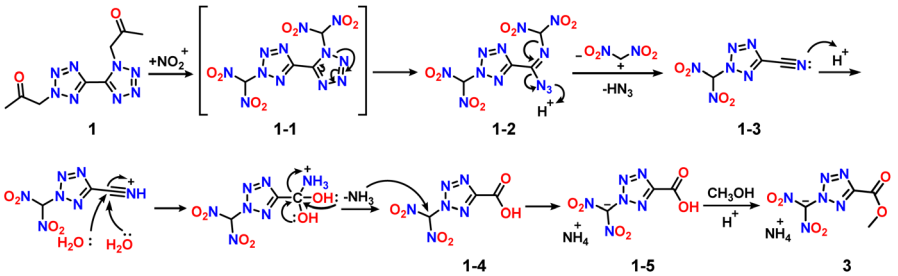

Scheme 2 Possible reaction processes of **3**.

Scheme 2. First, the methylene group at the 1,2-substituent position of compound **1** is attacked by nitronium to form an unstable dinitromethyl intermediate **1-1**. Initially, the N–N bond at the 1-substituted position on the tetrazole ring breaks due to its low bond energy, which results in the formation of intermediates **1-2**. Next, a series of intramolecular electron transfers occurred, leading to the removal of the dinitromethyl cation and azide. The azide ends up in the form of azidic acid under acidic conditions. 2-(Dinitromethyl)-2*H*-tetrazole-5-carbonitrile **1-3** is thus formed. Then, cyano is attacked twice by water molecules to undergo a hydrolysis reaction in a strong acid system. The hydroxyl group introduced during hydrolysis undergoes electron transfer, which leads to the removal of ammonia and the formation of 2-(dinitromethyl)-2*H*-tetrazole-5-carboxylic acid **1-4**. The stripped ammonia reacted with the dinitromethyl group to form an ammonium salt **1-5**. The final ammonium salt **1-5** is heated and stirred in a weak acid solution in methanol to undergo an esterification reaction, resulting in the formation of decomposition product dinitromethylammonium salt **3**. Since the environment for the esterification reaction is not very acidic, the ammonium ion is retained.

Single crystal X-ray structure analysis

Two polymorphs of **BDNBT** were confirmed by single-crystal X-ray diffraction and the differences in the molecular structure, packing styles and intermolecular interactions were investigated. **α-BDNBT** crystals (CCDC: 2336263 (193 K) and 2336254 (298 K)) and **β-BDNBT** crystals (CCDC: 2336247 (193 K)) were obtained by gradual evaporation of methanol at room temperature and 64 °C, respectively. The polymorph α of **BDNBT** belongs to the monoclinic space group $P2_1/n$ with two molecules per unit cell ($Z = 2$) and a crystal density of 1.917 g cm^{-3} at 193 K (Fig. 2a). The polymorph β of **BDNBT** crystallizes in the monoclinic space group $P2_1/c$ with four molecules per lattice cell ($Z = 4$) and has a crystal density of 1.899 g cm^{-3} at 193 K (Fig. 2b). As shown in Fig. 2c or Fig. 2d, the bistetrazole planar structure is also supported by torsion angles (N1–C1–C1a–N1a 180.00(1)° and C1–N2–N3–N4 −0.12(1)° in **α-BDNBT**; N1–N2–N3–N4 −0.4(7)° and N1–C1–C1_a–N1_a −180.0(5)° in **β-BDNBT**). In **α-BDNBT**, the dihedral angle between the dinitromethyl plane through N5–C2–N6 and the plane through the tetrazole ring is 87°. In **β-BDNBT**, the angles between the tetrazole and the two sets of dinitromethyl planes through N11–C4–N12 and N11A–C4–N12A are 87.9° and 79.9°, respectively. The structure of **α-BDNBT** is mainly dominated by intramolecular hydrogen bonding (C2–H2···O3) with a bond length of 2.59 Å (Fig. 2e). As shown in the green dashed portion of Fig. 2f, there is no intramolecular hydrogen bonding interaction in the structure of **β-BDNBT**, which is mainly dominated by intermolecular hydrogen bonding (C2–H2A···N10 and C4–H4A···N4), with bond lengths of 2.22 Å and 2.29 Å, respectively. In Fig. 2g and h, both **α-BDNBT** and **β-BDNBT** are stacked in a haphazard manner, but **α-BDNBT** is relatively neater than **β-BDNBT**. This also demonstrates why the **α-BDNBT** crystal density (1.917 g cm^{-3}) is higher than the **β-BDNBT** crystal density (1.899 g cm^{-3}).

Four molecules of the crystal **4**·CH_3OH fit into each unit cell as it crystallizes in the monoclinic $C2/m$ space group, where its measured density is 1.892 g cm^{-3} (193 K). Unlike the crystal **4**·CH_3OH, crystal **5** crystallizes in the monoclinic $P2_1/c$ space group with two molecules per unit and a measured density of 1.941 g cm^{-3} (223 K). As shown in Fig. 3e, the dinitromethyl plane through N5–C2–N5_d is perpendicular to the bistetrazole plane. Similar to **4**·CH_3OH, the two dinitromethyl groups of

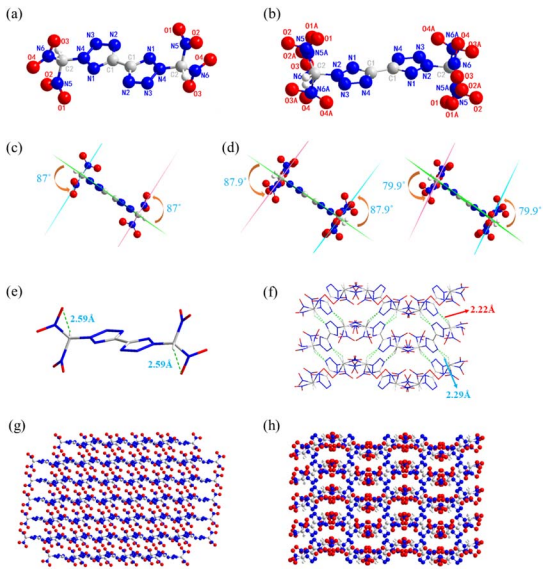

Fig. 2 (a) and (b) Molecular structure of **α-BDNBT** & **β-BDNBT**. (c) and (d) Planarity of **α-BDNBT** & **β-BDNBT**. (e) and (f) Hydrogen bonds of **α-BDNBT** & **β-BDNBT**. (g) and (h) Crystal packing diagram of **α-BDNBT** & **β-BDNBT**.

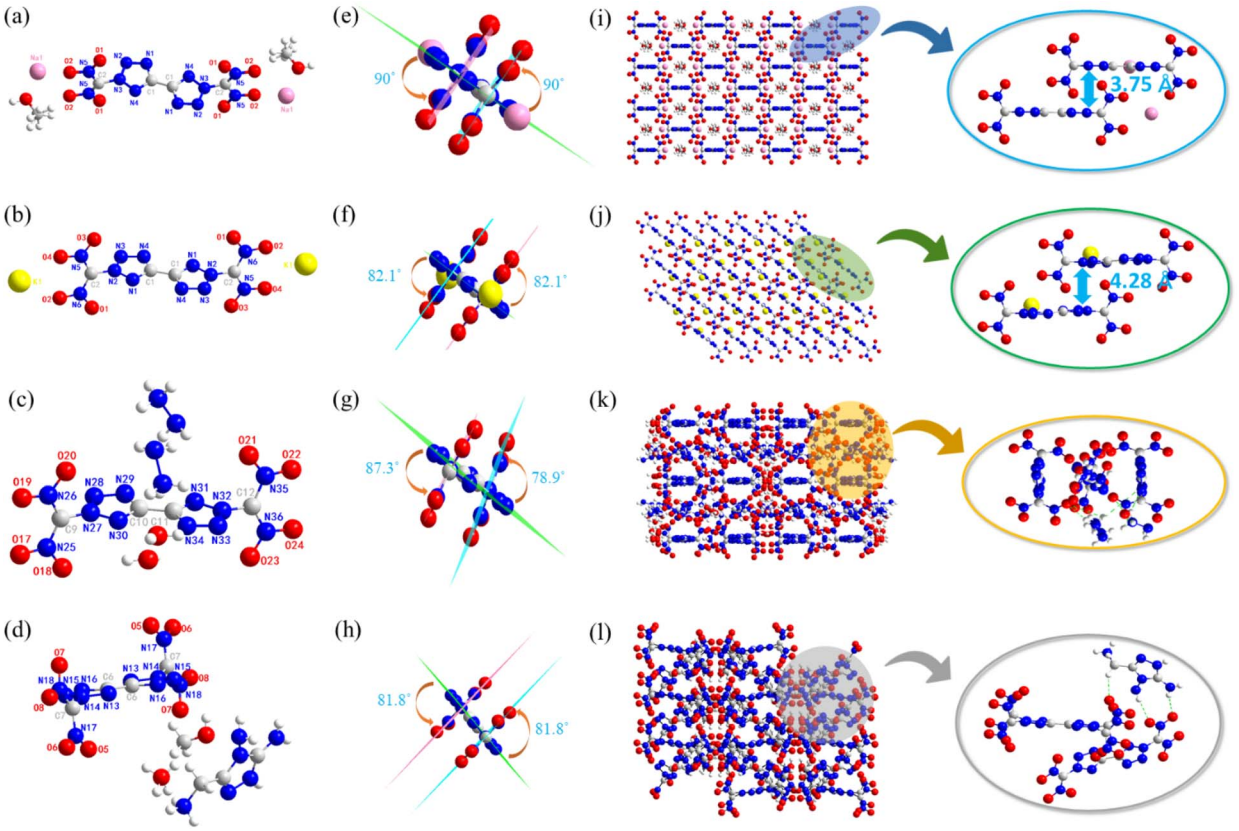

Fig. 3 (a)–(d) Molecular structure of **4**·CH_3OH, **5**, **7**·$2H_2O$, and **9**·CH_3OH H_2O. (e)–(h) Planarity of **4**·CH_3OH, **5**, **7**·$2H_2O$, and **9**·CH_3OH H_2O. (i)–(l) Crystal packing diagram of **4**·CH_3OH, **5**, **7**·$2H_2O$, and **9**·CH_3OH H_2O (the green dotted lines represent hydrogen bonds).

crystal **5** are almost perpendicular to the bistetrazole plane at an angle of 82.1° (Fig. 3f). It is possible that the large atomic radius of the potassium ion has deflected the dinitromethyl group. As shown in Fig. 3i or Fig. 3j, the crystal stacking systems of both crystals **4**·CH_3OH and crystals **5** exhibit layer-by-layer stacking with layer distances of 3.75 Å and 4.28 Å, respectively.

The crystal **7**·$2H_2O$ was measured at 193 K with a density of 1.761 g cm^{-3}. It crystalized in the monoclinic system and $C2/c$ space group. There are two molecules in one single unit cell ($Z = 2$). The crystal **9**·CH_3OH H_2O also belongs to the monoclinic $C2/c$ space group, but has four molecules per unit cell. Its crystal density at 218 K is 1.687 g cm^{-3}. Similar to the previous crystals, the two tetrazoles in crystal **7**·$2H_2O$ also remain in the same plane (N9–N10–C3–C2 −176.8(5) and N4–N5–C2–C3 −179.4(5)). However, the two dinitromethyl planes through N25–C9–N26 and N35–C12–N36 in crystal **7**·$2H_2O$ are not parallel. Different from **7**·$2H_2O$, the two dinitromethyl planes in crystal **9**·CH_3OH H_2O are parallel and the dinitromethyl group has an angle of 81.8° with the bistetrazole plane (Fig. 3h). As shown in Fig. 3g, the angles between these two planes and the bistetrazole plane are 87.3° and 78.9°, respectively. In addition, **7**·$2H_2O$ exhibits a composite stacking and intermolecular hydrogen bonds involving N41–H41A···O14, N38–H38A···N29 and N45–H45B···O22 are observed (Fig. 3k). Similarly, crystal **9**·CH_3OH H_2O exhibits a composite stacking and intermolecular hydrogen bonds (N8–H8···O1, O9–H9A···N12, and C8–H8A···O9).

Physicochemical and energetic properties

The physicochemical and energetic properties of **α-BDNBT**, **β-BDNBT** and energetic salts **4–10** are summarized in Table 1.

The densities of all compounds were measured using a gas hydrometer at 25 °C in a helium (He) atmosphere. Compounds were dried in an oven at 30 °C to remove the solvents completely, as evidenced by DSC curves. The densities of **BDNBT** and its derivatives ranged from 1.813 to 1.922 g cm^{-3}, which are higher than those of RDX (1.805 g cm^{-3}) (Table 1). The Gaussian 09 program was used to calculate the heats of formation (ΔH_f) for **BDNBT** and its derivatives, which ranged from 0.19 to 3.82 kJ g^{-1}. The heat of formation for all target compounds, except for the potassium salt **7** ($\Delta H_f = 0.19$ kJ g^{-1}), was much greater than that of RDX ($\Delta H_f = 0.36$ kJ g^{-1}) and HMX ($\Delta H_f = 0.25$ kJ g^{-1}). Detonation velocities and pressures were predicted using EXPLO5 v6.01 based on measured densities and the calculated heat of formation of **BDNBT** and its derivatives.[21] **α-BDNBT** maintains a high density of 1.880 g cm^{-3} and outstanding detonation performance ($D = 9480$ m s^{-1} and $P = 40.2$ GPa), with a total nitrogen and oxygen content of 85.54% and a near-zero oxygen balance (OB = −4.62%). Although **β-BDNBT** has slightly inferior performance compared with **α-BDNBT**, it still exhibits higher detonation performance ($D = 9306$ m s^{-1} and $P = 38.5$ GPa) than the commonly used explosives RDX ($D = 8795$ m s^{-1} and $P = 34.9$ GPa) and HMX ($D =$

Table 1 The physicochemical and energetic properties of α, β-BDNBT and compounds 4–10

Comp.	ρ^a (g cm^{-3})	$\Delta_f H_m{}^b$ (kJ mol^{-1}/kJ g^{-1})	D^c (m s^{-1})	P^d (GPa)	$OB_{CO_2}{}^e$ (%)	N + O^f (%)	$T_m{}^g$ (°C)	$T_d{}^h$ (°C)	IS^i (J)	FS^j (N)
α-BDNBT	1.880^k	838.8/2.42	9480	40.2	−4.62	85.54	—	91	4	40
β-BDNBT	1.863	838.8/2.42	9306	38.5	−4.62	85.54	—	84	3	28
4	1.915	343.4/0.88	7882	27.1	−4.10	75.90	—	142	3	32
5	1.922	223.1/0.19	7955	28.6	−3.79	70.11	—	222	<1	<5
6	1.813	484.4/1.27	8966	35.2	−16.83	85.24	—	121	6	60
7	1.822	759.1/1.85	9224	37.2	−19.50	85.83	—	145	5	60
8	1.891	617.4/1.50	9503	41.1	−7.76	86.38	—	124	5	60
9	1.824	1815.1/3.82	9413	39.3	−37.10	80.15	97	138	9	108
10	1.904	1639.9/3.25	9612	42.8	−25.38	81.73	—	146	10	120
RDX^l	1.805	80.0/0.36	8795	34.9	−21.6	81.06	—	204	7.4	120
HMX^m	1.905	104.8/0.25	9144	39.2	−21.6	81.06	—	280	7.4	120

^{a} Measured densities using a gas pycnometer at 25 °C. ^{b} Calculated molar enthalpy of formation. ^{c} Calculated detonation velocity. ^{d} Calculated detonation pressure. ^{e} Oxygen balance (based on CO_2). ^{f} Nitrogen and oxygen contents in %. ^{g} Melting temperature (onset). ^{h} Decomposition temperature (onset). ^{i} Impact sensitivity. ^{j} Friction sensitivity. ^{k} Crystal density at 298 K. ^{l} Ref. 23. ^{m} Ref. 24.

9144 m s^{-1} and P = 39.3 GPa). Energetic ionic salts **4** and **5** are metal salts with advantages in density, measuring 1.915 g cm^{-3} and 1.922 g cm^{-3}, respectively. Energetic potassium salts **5** shows a significant improvement in thermal decomposition temperature (T_d = 222 °C), which is the highest among that of all salt compounds. Compared with **α-BDNBT** (D = 9480 m s^{-1}, P = 40.2 GPa; T_d = 91 °C; IS = 4 J, and FS = 40 N), the energetic ammonium salt **6** shows low sensitivity (IS = 6 J and FS = 60 N), the energetic hydrazine salt **7** displays a high thermal decomposition temperature (T_d = 145 °C), and the energetic hydroxylamine salt **8** exhibits a high detonation performance (D = 9503 m s^{-1} and P = 41.1 GPa). Divalent high-energy salts **9** and **10** have achieved breakthroughs in detonation performance (**9**: D = 9413 m s^{-1} and P = 39.3 GPa; **10**: D = 9612 m s^{-1} and P = 42.8 GPa) and sensitivity (**9**: IS = 9 J and FS = 108 N; **10**: IS = 10 J and FS = 120 N). Aside from the energy properties, the friction sensitivity (FS) and impact sensitivity (IS) measured using the standard BAM methods are also of great interest.[22] Compound **10** (FS = 120 N) exhibits friction sensitivity similar to that of HMX and RDX, while its impact sensitivity (IS = 10 J) is superior to that of HMX (IS = 7.4 J) and RDX (IS = 7.4 J).

To investigate the difference between the thermal stability of **α-BDNBT** and **β-BDNBT**, differential scanning calorimetry (DSC) measurements were carried out in a nitrogen atmosphere at a linear heating rate of 5 °C min^{-1}. The onset decomposition temperature of **β-BDNBT** is 84 °C with a peak temperature of 89 °C (Fig. 4). The onset decomposition temperature of **α-BDNBT** is 91 °C, which is slightly higher than that of **β-BDNBT** (T_{onset} = 84 °C). It is noteworthy that the decomposition peak widths of **α-BDNBT** and **β-BDNBT** are almost the same at 10 °C, which confirms the rapid energy release rate and strong detonation performance of **BDNBT**.

Similarly, monovalent cationic salts of **BDNBT**, such as sodium salt **4**, potassium salt **5**, ammonium salt **6**, hydrazine salt **7**, hydroxylamine salt **8**, and divalent cationic salts, such as 4,5-diamino-3-(aminomethyl)-4*H*-1,2,4-triazolium salt **9**, and 2,4,6-triamino-1,3-dihydroxy-1,3,5-triazinane-1,3-diium salt **10**, were also characterized with regard to their thermal decomposition temperatures. The decomposition temperature profile waterfall plots are shown in Fig. 5. The decomposition temperatures of these salts range from 121–146 °C, except for the energetic potassium salt **5**, with a decomposition temperature of 222 °C. This is generally consistent with our common perception that dinitromethyl compounds have low

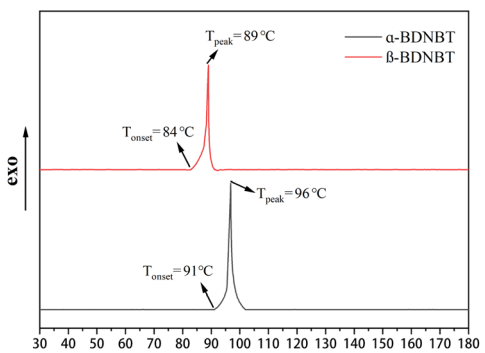

Fig. 4 DSC plots of α and β-BDNBT.

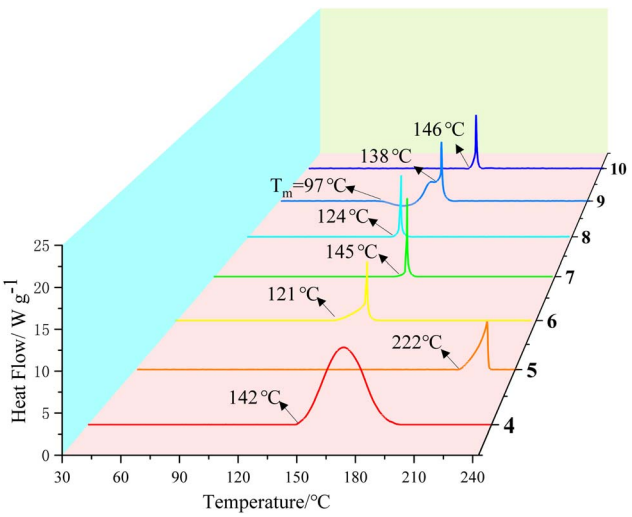

Fig. 5 DSC plots of 4–10.

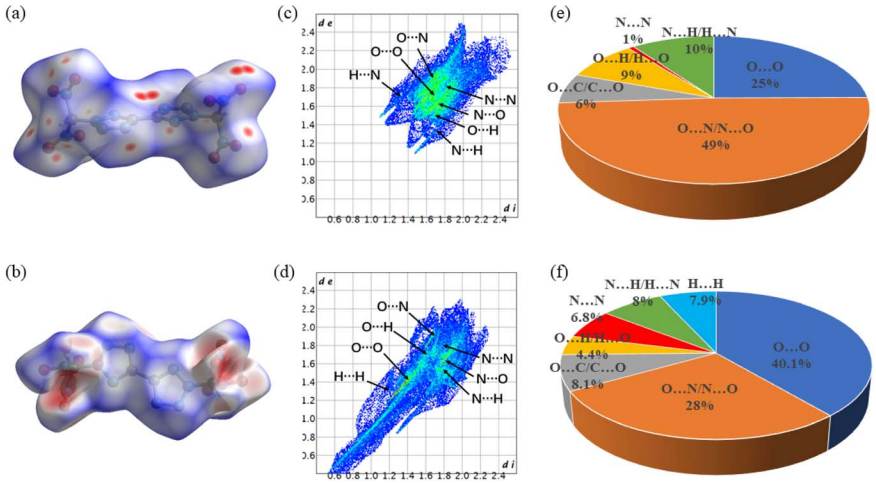

Fig. 6 (a) and (b) Hirshfeld surfaces in crystal stacking for **α** and **β-BDNBT**. (c) and (d) 2D fingerprint plot for **α** and **β-BDNBT**. (e) and (f) The pie graph for **α** and **β-BDNBT** shows the percentage contributions of the individual atomic contacts to the Hirshfeld surface.

decomposition temperatures. Energetic salt **9** has melting point due to the presence of a methylene component in its cation with a starting melting temperature of 97 °C.

As shown in Table 1, **α-BDNBT** exhibits lower sensitivity than **β-BDNBT**, which may be related to intermolecular forces. To gain more insight into the intermolecular interactions, the two-dimensional (2D) fingerprints of **α-BDNBT** and **β-BDNBT** crystals and the associated Hirshfeld surfaces were analyzed using Crystalexplorer 17.5 (Fig. 6).[25] The red and blue regions on the Hirshfeld surfaces represent the high and low contact groups, respectively.[26] As shown in Fig. 6a and b, the red dots in **α-BDNBT** are scattered on various parts of the molecule, in which N···O and O···N interactions are the strongest, while the red dots in **β-BDNBT** are scattered on the molecule mainly close to the dinitromethyl group, with the largest proportion of O···O bonds. The proportion of O···O bonds in **β-BDNBT** is 40.1%, higher than that of **α-BDNBT** (25%), which might be related to the fact that **β-BDNBT** is more sensitive than **α-BDNBT**.

Conclusions

In conclusion, two polymorphic forms (α and β) of bistetrazole and seven energetic salts were synthesized and characterized using a strategy involving the co-assembly of dinitro and bistetrazole. This strategy effectively addresses the issue of high sensitivity in bistetrazole derivatives. Among them, the structures of **α-BDNBT**, **β-BDNBT**, **4**·CH_3OH, **5**, **7**·$2H_2O$, and **9**·CH_3OH H_2O are confirmed by single crystal X-ray diffraction. The neutral compound **α-BDNBT** has a crystal density of up to 1.880 g cm^{-3} (298 K) and excellent detonation properties (D = 9480 m s^{-1} and P = 40.2 GPa), superior to those of the conventional explosives RDX (D = 8795 m s^{-1} and P = 34.9 GPa) and HMX (D = 9144 m s^{-1} and P = 39.3 GPa). Furthermore, **α-BDNBT** shows superior oxygen balance (OB% = −4.62%) and lower friction sensitivity (FS = 40 N) compared with other tetrazole derivatives (FS < 5 N). Within the energetic salts (**4–10**) derived from **BDNBT**, energetic potassium salts **5** boast the highest density and thermal decomposition temperature (ρ = 1.922 g cm^{-3} and T_d = 222 °C), energetic 2,4,6-triamino-1,3-dihydroxy-1,3,5-triazine-1,3-diium salts **10** display superior detonation performance (D = 9612 m s^{-1} and P = 42.8 GPa) and the lowest sensitivity (IS = 10 J and FS = 120 N). The results demonstrate that **BDNBT** and its energetic salts have high densities (1.813–1.922 g cm^{-3}) and exhibit excellent detonation performance (7882–9612 m s^{-1}), indicating their potential as a novel type of high-energy density material (HEDM).

Data availability

All data supporting the findings of this study are available within the article and its ESI.†

Conflicts of interest

The authors declare no competing financial interest.

Acknowledgements

This work was supported by the National Natural Science Foundation of China (No. 22075143 and 22205110), the Natural Science Foundation of Jiangsu Province (BK20220958), and the Fundamental Research Funds for the Central Universities (30922010404).

References

1 T. M. Klapötke, M. Kofen and J. Stierstorfer, N-Functionalisation of 5,5′-bistetrazole providing 2,2′-di(azidomethyl)bistetrazole: a melt-castable metal-free green primary explosive, *Dalton Trans.*, 2021, **50**, 13656–13660.

2 N. Fischer, D. Izsák, T. M. Klapötke, S. Rappenglück and J. Stierstorfer, Nitrogen-rich 5,5′-bistetrazolates and their

potential use in propellant systems: a comprehensive study, *Chem.–Eur. J.*, 2012, **18**, 4051–4062.
3 D. Fischer, T. M. Klapötke, J. Stierstorfer and N. Szimhardt, 1,1′-Nitramino-5,5′-bitetrazoles, *Chem.–Eur. J.*, 2016, **22**, 4966–4970.
4 T. M. Klapötke, D. G. Piercey and J. Stierstorfer, Amination of energetic anions: high-performing energetic materials, *Dalton Trans.*, 2012, **41**, 21–31.
5 M. Benz, T. M. Klapötke and J. Stierstorfer, Krapcho Decarboxylation of ethyl-carbazate: synthetic approach toward 1,1′-diamino-5,5′-bistetrazole and its utilization as a high-performing metal-free initiator, *Org. Lett.*, 2022, **24**, 1747–1751.
6 N. Fischer, L. Gao, T. M. Klapötke and J. Stierstorfer, Energetic salts of 5,5′-bis(tetrazole-2-oxide) in a comparison to 5,5′-bis(tetrazole-1-oxide) derivatives, *Polyhedron*, 2013, **51**, 201–210.
7 X. Wang, S. Jin, C. Zhang, L. Li, S. Chen and Q. Shu, Preparation, Crystal structure and properties of a new crystal form of diammonium 5,5′-bistetrazole-1,1′-diolate, *Chin. J. Chem.*, 2015, **33**, 1229–1234.
8 N. Fischer, D. Fischer, T. M. Klapötke, D. G. Piercey and J. Stierstorfer, Pushing the limits of energetic materials – the synthesis and characterization of dihydroxylammonium 5,5′-bistetrazole-1,1′-diolate, *J. Mater. Chem. A*, 2012, **22**, 38–50.
9 W. Hu, J. Tang, X. Ju, Z. Yi, H. Yang, C. Xiao and G. Cheng, An efficient one-step reaction for the preparation of advanced fused bistetrazole-based primary explosives, *ACS Cent. Sci.*, 2023, **9**, 742–747.
10 T. Yan, H. Yang, C. Yang, Z. Yi, S. Zhu and G. Cheng, An advanced and applicable heat-resistant explosive through controllable regiochemical modulation, *J. Mater. Chem. A*, 2020, **8**, 23857–23865.
11 C. Lei, G. Cheng, Z. Yi, Q. Zhang and H. Yang, A facile strategy for synthesizing promising pyrazole-fused energetic compounds, *Chem. Eng. J.*, 2021, **416**, 129190.
12 J. Singh, R. J. Staples and J. M. Shreeve, Manipulating nitration and stabilization to achieve high energy, *Sci. Adv.*, 2023, **9**, eadk3754.
13 Q. Yu, P. Yin, J. Zhang, C. He, G. H. ImLer, D. A. Parrish and J. M. Shreeve, Pushing the limits of oxygen balance in 1,3,4-oxadiazoles, *J. Am. Chem. Soc.*, 2017, **139**, 8816–8819.
14 M. A. Kettner and T. M. Klapötke, 5,5′-Bis-(trinitromethyl)-3,3′-bi-(1,2,4-oxadiazole): a stable ternary CNO-compound with high density, *Chem. Commun.*, 2014, **50**, 2268–2270.
15 X. X. Zhao, S. H. Li, Y. Wang, Y. C. Li, F. Q. Zhao and S. P. Pang, Design and synthesis of energetic materials towards high density and positive oxygen balance by N-dinitromethyl functionalization of nitroazoles, *J. Mater. Chem. A*, 2016, **4**, 5495–5504.
16 N. V. Muravyev, K. Y. Suponitsky, I. V. Fedyanin, I. V. Fomenkov, A. N. Pivkina and I. L. Dalinger, Bis-(2-difluoroamino-2,2-dinitroethyl) nitramine – energetic oxidizer and high explosive, *Chem. Eng. J.*, 2022, **449**, 137816.
17 L. Hu, P. Yin, G. Zhao, C. He, G. H. ImLer, D. A. Parrish, H. Gao and J. M. Shreeve, Conjugated energetic salts based on fused rings: insensitive and highly dense materials, *J. Am. Chem. Soc.*, 2018, **140**, 15001–15007.
18 C. He and J. M. Shreeve, Potassium 4,5-bis(dinitromethyl) furoxanate: a green primary explosive with a positive oxygen balance, *Angew. Chem., Int. Ed.*, 2016, **55**, 772–775.
19 J. Zhang, S. Dharavath, L. A. Mitchell, D. A. Parrish and J. M. Shreeve, Energetic salts based on 3,5-bis(dinitromethyl)-1,2,4-triazole monoanion and dianion: controllable preparation, characterization, and high performance, *J. Am. Chem. Soc.*, 2016, **138**, 7500–7503.
20 E. Oliveri-Mandala and T. Passalacqua, Bistetrazole and isomeric derivatives of tetrazole, *Gazz. Chim. Ital.*, 1914, **43**, 465–475.
21 C. Li, T. Zhu, C. Lei, G. Cheng, C. Xiao and H. Yang, Construction of p-nitropyrazole-1,3,4-triazole framework energetic compounds: towards a series of high-performance heat-resistant explosives, *J. Mater. Chem. A*, 2023, **11**, 12043–12051.
22 E. R. Johnson, S. Keinan, P. Mori-Sánchez, J. Contreras-García, A. J. Cohen and W. Yang, Revealing noncovalent interactions, *J. Am. Chem. Soc.*, 2010, **132**, 6498–6506.
23 C. Li, T. Zhu, J. Tang, G. Yu, Y. Yang, H. Yang, C. Xiao and G. Cheng, Trinitromethyl groups-driven fused high energy compound featuring superior comprehensive performances, *Chem. Eng. J.*, 2024, **479**, 147355.
24 J. Li, Y. Liu, W. Ma, T. Fei, C. He and S. Pang, Tri-explosophoric groups driven fused energetic heterocycles featuring superior energetic and safety performances outperforms HMX, *Nat. Commun.*, 2022, **11**, 2837.
25 M. A. Spackman and J. J. McKinnon, Fingerprinting intermolecular interactions in molecular crystals, *CrystEngComm*, 2002, **4**, 378–392.
26 J. Zhang, Q. Zhang, T. T. Vo, D. A. Parrish and J. M. Shreeve, *J. Am. Chem. Soc.*, 2015, **137**, 1697–1704.

